Journal of Intelligent & Robotic Systems
https://doi.org/10.1007/s10846-019-01105-y

Aerial Wilderness Search and Rescue with Ground Support

Zendai Kashino [1] · Goldie Nejat [1] · Beno Benhabib [1]

Received: 25 June 2019 / Accepted: 20 September 2019

Abstract
Unmanned aerial vehicles (UAVs) have been proposed for a wide range of applications. Their use in wilderness search and rescue (WiSAR), in particular, has been investigated for fast search-area coverage from a high vantage point. The probability of success in such searches, however, can be further improved utilizing cooperative systems that employ both UAVs and unmanned ground vehicles (UGVs). In this paper, we present a new coordinated-search planning method, for collaborative UAV-UGV teams. The proposed method, particularly developed for WiSAR, considers the search area to be continuously growing and that the search is sparse. It is also assumed that targets detected by UAVs must be identified by a ground-level searcher. The UAV/UGV motion-planning method presented herein, therefore, has two major components: (*i*) coordinated search and (*ii*) joint target identification. The novelty of the proposed method lies in its use of (*i*) time-dependent target-location iso-probability curves, and (*ii*) an effective and efficient coordinated target-identification algorithm. The method has been validated via numerous simulated WiSAR searches for varying scenarios. Furthermore, extensive comparative experiments with other methods have shown that our method has higher rates of target detection and shorter search times, significantly outperforming alternative techniques by 75% – 255% in terms of target detection probability.

Keywords Autonomous mobile-target search · UAV-UGV Cooperative search planning · Iso-probability curves · Wilderness search and rescue

1 Introduction

Unmanned aerial vehicles (UAVs) have been used in a variety of fields [1–6], including search and rescue (SAR) [7–20]. The SAR literature has, primarily, focused on three sub-areas of research: the overall evaluation of UAV systems and their possible integration with ground/ surface search teams [16–20], the planning of UAV search trajectories [7–13], and the detection of targets in aerial images [14, 15]. Search-trajectory planning has been particularly challenging due to the large and often growing search space and inherent uncertainty regarding the target's potential whereabouts. Similarly, identifying targets in aerial images has been difficult due to the uncertainty of what features should be looked for in order to identify a target. For example, in [14], it was claimed that up to 90% of the UAV detections can be subjects other than the searched targets (*i.e.*, false positives).

✉ Beno Benhabib
benhabib@mie.utoronto.ca

[1] University of Toronto, 5 King's College Road, Toronto, ON M5S 3G8, Canada

Although the performance of (stand-alone) UAVs is key to successful SAR missions, the chances of finding the searched target can be significantly improved via *cooperative systems* employing both UAVs and unmanned-surface (USV) or -ground (UGV) vehicles [21–43]. Such cooperative systems have been widely considered for urban SAR (USAR) (*e.g.*, [24]), wilderness SAR (WiSAR) (*e.g.*, [23]), and air-sea rescue (ASR) operations (*e.g.*, [25]). In this paper, our specific focus is on search trajectory planning for cooperative UAV-UGV systems configured for WiSAR.

In [37], UAVs and UGVs were coordinated using a distributed digital pheromone-based swarming approach. In this approach, 'pheromones' are digital annotations over the search area denoting areas that have yet to be searched, possible target locations, no-go zones, and areas planned to be searched by other vehicles. Each search agent maintains its own pheromone map defined over the search area and plans a finite horizon path to maximize a pheromone-dependent objective function. In [38], UAVs are used to, first, obtain rough estimates of target locations, followed by a refinement of the estimates by UGVs. The UAV search path is planned using either a fixed search pattern or a reactive information-gathering motion controller. While the latter is also applicable to UGVs, the UGV's motion is primarily controlled by a

Published online: 22 November 2019

similar reactive controller for reducing the uncertainty of feature location estimates. In [39], search was formulated as a multi-robot task allocation problem while considering that some units, like UAVs, are used for locating targets, while other units, such as UGVs, identify and rescue targets. Hindsight optimization is used in an on-line planning approach to assign tasks to each robot in the face of uncertainty.

In [40], an auction-based task allocation approach was proposed to plan a search. Namely, tasks (auction items) are given to search agents (bidders) with the maximum expected utility to be gained from carrying out the task (the bid). The expected utility gained by an agent carrying out a task is the expected value of the reward of finding the target less the cost of inserting the task into its current task list. In [41], an agent-control architecture, named the *hybrid intelligent control agent*, was proposed. This architecture combines continuous-state control and discrete-state based control into a hybrid system. The controller was demonstrated for a UAV-UGV search and capture mission. In [42], the search planning problem over a set of grid cells was formulated as a mixed-integer linear program (MILP). The search planning is treated as an optimization problem of finding a set of search paths to maximize coverage and connectivity. Ways in which to incorporate constraints on both instantaneous connectivity and recurrent connectivity (over time) into the MILP framework are presented.

In [43], a cooperative approach to search trajectory planning is presented for a USAR setting. The work considers cooperative localization and tracking of a mobile target in an urban environment using a distributed auction scheme and path planning trees to plan finite look-ahead paths. Both UAVs and UGVs are considered to be able to locate and track the target.

Our work, presented herein, uniquely considers a collaborative UAV-UGV team carrying out a coordinated search in a growing and sparse (search) area (*i.e.*, the entire growing search area cannot be investigated given the available time and resources). The UAVs carry out an aerial search and the UGVs conduct the ground search, respectively. While other works typically assume that UAVs or UGVs can identify targets, even though the UAVs may detect and locate targets more efficiently than the UGVs, they cannot positively confirm their identities. Occlusion due to foliage and weather, for example, can make it difficult for UAVs to identify targets from above. UGVs, on the other hand, are assumed to be able to do both, namely, carry out an independent search for the target as well as 'help' in the identification of targets detected by the UAVs. Thus, the novel UAV/UGV motion-planning method presented in this paper allows for coordinated search and joint identification for lost targets in WiSAR using heterogeneous sensing capabilities.

In the proposed method, specifically, both the UAVs and UGVs search for the target using iso-probability curves, which were first introduced in [44], to model the (untracked) target motion. Our initial work which developed a UAV-only search-planning method using iso-probability curves was detailed in [45]. In contrast to previous uses of the iso-probability curves, in which UGVs were assigned to and must follow individual curves for the duration of the search [46], our new proposed approach allows the UAVs to traverse and cover a range of iso-probability curves optimally and in coordination with the UGVs' search. The new approach allows UAVs to cover all possible target motions, without bias towards any particular target motion, while also avoiding search redundancies when searching with UGVs.

2 The WiSAR Problem

This paper focuses on addressing the mobile-target search problem in the context of WiSAR using a UAV search team supported by UGVs. A detailed description of the problem is presented below.

2.1 Planning Problem

The wilderness-search planning problem addressed herein is one of maximizing the probability of successfully locating a lost person given a finite amount of search resources (UAVs and UGVs). Addressing this problem requires coordinating the search resources effectively using the available incomplete and probabilistic information regarding the target and the search region.

Target data available at the start of the search is, typically, limited to their last known position (LKP) (*e.g.*, the trail head from which they intended to start their hike) and their demographic data (*e.g.*, hiker, biker, child, adult, young, old, etc.). It is important to note that the target's real-time location is unknown and untrackable throughout the search until detection. Similarly, only global terrain information is available before the search. Thus, UAVs and UGVs need to deal with specific terrain information and target-clues found during the search in real-time.

Numerous wilderness target-motion prediction models have been considered in the literature (e.*g.*, [47–51]). Herein, the motion model assumes the target wanders randomly: maintaining a fixed heading for a random distance before choosing a new random heading to travel along. Motion is, thus, specified by a series of random headings and distances. Two parameters are used to characterize the target motion: σ_θ and $d_{\max}$, [48]. The former, σ_θ, is the standard deviation of the normal distribution from which possible headings that the

target will take are drawn. The latter, $d_{\max}$, is the upper bound of a uniform distribution from which target travel distances are drawn (*i.e.*, the distance the target will travel before randomly deciding on a new one). Both are defined as.

$$\theta_i \sim N(\mu = \theta_t, \sigma = \sigma_\theta), \text{and } d_i \sim U(0, d_{max}), \quad (1)$$

where (θ_i, d_i) represent the i^{th} segment (heading and distance) travelled by the target since starting its motion at the LKP, respectively.

Above, σ_θ characterizes the degree to which the target wanders around, while $d_{\max}$ is a measure of the target's indecisiveness. One could note that both σ_θ and $d_{\max}$ can be inferred, along with a probability distribution defining possible target walking speeds, from demographic information and historical WiSAR data [52]. Figure 1 shows an example in which the target has just completed the end of its 4th segment and is about to embark on its 5th, where d_t and θ_t represent the target's current (absolute) location with respect to the LKP.

The generated target path is used in conjunction with a terrain model (*e.g.*, vegetation, slope, etc.), to determine target trajectories. Since the target is mobile, the search area increases in size over time.

Regarding UAV and UGV capabilities, in this work, we assume a binary disk model of target detection for both search agents. Namely, it is assumed that a target is detected if it is within the detection circle of the search agent, defined by r_a or r_g for UAVs or UGVs, respectively:

$$|\mathbf{x}_a - \mathbf{x}_t| \le r_a \text{ or } |\mathbf{x}_g - \mathbf{x}_t| \le r_g, \quad (2)$$

where $\mathbf{x}_a$ is any UAV's position, $\mathbf{x}_g$ is any UGV's position, and $\mathbf{x}_t$ is the target's position at a given time. Other assumptions include the following: (*a*) UAVs cannot detect targets under tree cover; (*b*) targets detected by UAVs must be checked by a UGV for confirmation of identity; (*c*) all UAVs and UGVs have access to a global communication network connected to a central coordinator, which relays changes to the search plan and any coordination between UAVs and UGVs instantaneously; and, (*d*) the search team

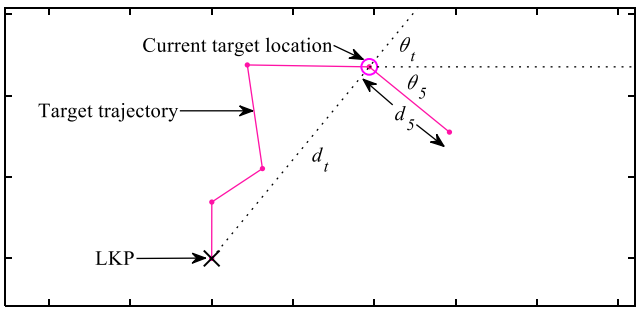

Fig. 1 An example target trajectory with the target having completed travel along 4 headings so far. Variables are shown for the 5th heading

arrives at the target LKP sometime after the target has left it, at t_{start}, and that the search is carried out until a predetermined *end of search time*, t_{end}.

2.2 Problem Formulation

The goal in planning a search for a lost target is to maximize the probability of a success (POS), defined herein as the product of the probability of the target being in a considered area (POA) and the probability of detecting the target (POD), if it were in the area [52]:

$$\text{POS} = \text{POA} \times \text{POD}. \quad (3)$$

POA can be defined by a bivariate continuous random variable denoting target position, $\mathbf{X}_t$. For any area A of the search area, then, the POA is the probability that $\mathbf{X}_t$ is in A:

$$\text{POA} = P(\mathbf{X}_t \in A). \quad (4)$$

Similarly, POD can be defined by a binary random variable, D, which denotes target detection if search resources are allocated to the search area A. The POD is, then, the probability of a successful detection given that the target is in A:

$$\text{POD} = P(D = \text{success} | \mathbf{X}_t \in A). \quad (5)$$

The POS is, therefore, the probability of the target being in area A and the target being found, *i.e.*, the probability of successful target detection:

$$\text{POS} = P(D = \text{success}, \mathbf{X}_t \in A). \quad (6)$$

Determining the overall probability of successful target detection during a search, then, requires summing the POS values across all areas over the duration of the search. However, one must note that (*i*) POA is a function of time, and (*ii*) POD depends on where the searchers are directed to search (*i.e.*, the UAV and UGV trajectories). Characteristics of an effective search strategy, thus, can be extracted by considering several characteristics of the POD with respect to search effort allocation.

If the POD increases proportionally to the search effort allocated, maximizing the total POS has a greedy solution. Namely, an optimal strategy would call for exhaustively searching areas, while prioritizing areas with higher POA. In a dynamic problem, however, there are diminishing returns, as an increasing amount of search effort is spent in an area. Namely, the increase in POD per unit of search effort allocated decreases as more effort is allocated to an area. In this case, an optimal search strategy would call for diversifying the allocation of search effort, exploring a range of possible target locations instead of exhaustively searching where the target is

most probably located. A search, balancing exploitation and exploration, can be planned by allocating search effort proportionally to the POA at any time. This allocates more search effort where the target is more likely to be while ensuring all possible target locations are searched.

One may note, however, that search effort cannot be distributed throughout the search area and is continuously reconfigured to exactly match the dynamic POA of the mobile target. Namely, a finite number of searchers (*i.e.*, UAVs and UGVs) must travel through the search area looking for the target at a finite velocity with a finite detection radius. Planning UAV/UGV trajectories, to search the time-varying POA such that effort is allocated proportionally to the POA at all times, would not be feasible.

It is, thus, assumed here that searching all possible targets with an equal amount of search effort would similarly lead to an optimal search that balances exploitation and exploration. Namely, even with a mobile target, all possible target motions could be searched with equal effort to obtain the desired effect. Therefore, in this paper, we address the problem of maximizing the POS by planning a search that considers all possible target motions with equal effort. One way of expressing this approach is to formulate the range of possible targets as a univariate probability distribution function (PDF). In such a case, an equal effort search can be achieved by making the percentile target being searched proportional to the search effort expended throughout the search:

$$p(t) \propto E(t), \tag{7}$$

where $p(t)$ is the target percentile being searched at time t, and $E(t)$ is the time-cumulative effort spent up to time t.

Furthermore, in our case of UAV/UGV search, the problem of coordination must be considered. As abovementioned, UAVs require a UGV to identify any targets they detect. Timely identification of these targets is vital for an effective search. Late confirmations can result in wasted time. Namely, time spent by UAVs tracking a detected (false) target until identification by a UGV could have been spent searching for the real target. Thus, UGV motion planning should have a secondary objective of minimizing interception time, in addition to maximizing the probability of target detection.

A metric that can be used to quantify *the time to identification* by a UGV is the minimum distance between the UAV and its nearest UGV:

$$d_{ga} = \min\left(\|\mathbf{x}_g(t) - \mathbf{x}_a(t)\|\right), \tag{8}$$

where $\mathbf{x}_g$ is the position of UGV g and $\mathbf{x}_a$ is the position of UAV a.

3 Background Information

The proposed search planning method utilizes several concepts developed in our previous works. This section provides a brief overview of these.

3.1 Iso-Probability Curves

Iso-probability curves are closed curves that encircle the target's LKP [44]. At any given time, they denote the farthest the P^{th} percentile target could reach in any given direction since leaving the LKP. Figure 2 shows a set of three iso-probability curves (10%, 50%, and 90%, respectively) at two different times (t and $t + \Delta t$).

In the work presented in this paper, iso-probability curves are used to guide both UAV and UGV search trajectories. UAVs are assigned to search a range of iso-probability curves with equal effort spent on each, while UGVs are assigned to search a fixed set of iso-probability curves for the duration of the search.

3.2 Pseudo-Redundant Coverage

Redundant coverage, for static targets, is defined as revisiting locations that have already been searched. Avoiding such redundant coverage would, naturally, improve the efficiency of search. However, mobile targets can move back into locations that have already been searched. As such, true redundant coverage does not exist in a mobile-target search. Herein, *pseudo-redundant coverage*, a dynamic analog to redundant coverage, is addressed [45].

Pseudo-redundant coverage refers to revisiting a confidence area [10] – a region within which one is confident that the target is not present. This confidence area shrinks over time. Namely, as time passes, targets have higher probability to return into areas that have already been searched.

A search agent's trajectory and the confidence area around it, at time t, are shown in Fig. 3. Several previous discrete

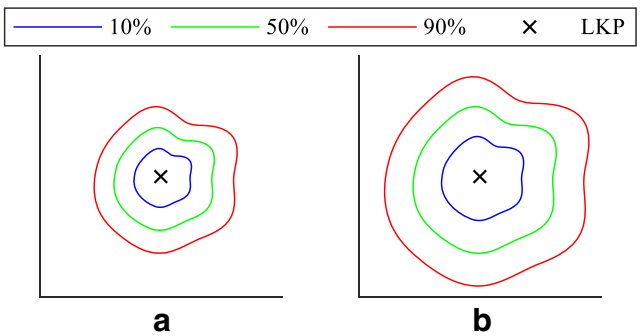

Fig. 2 A set of iso-probability curves at **a** t, and **b** $t + \Delta t$

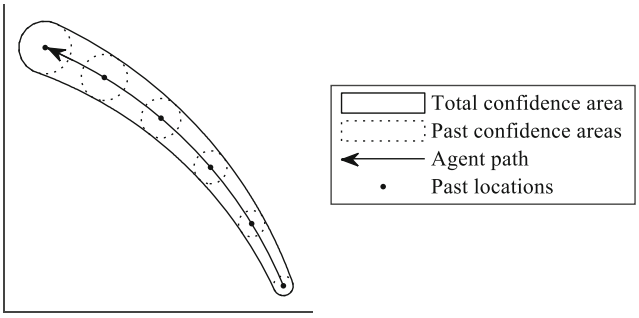

Fig. 3 A search path and the associated confidence area

positions are marked on the trajectory with corresponding circular confidence areas, respectively. The total confidence area (bounded by the outer solid line) is the union of all past confidence areas around all locations the searcher has passed through. As one may note, the confidence area circles, at past times, have shrank from their original size (equal to the last one shown).

4 Proposed Search Method

The proposed approach to robotic WiSAR consists of three phases: search-agent trajectory planning, joint target identification, and search-agent trajectory re-planning. The first phase pertains to planning UAV/UGV search trajectories to maximize their probability of detecting the target. The second phase is triggered when a potential target is detected by a UAV and a UGV is dispatched to identify it. The third phase is initiated when new information regarding the target (*e.g.*, a clue) is detected leading to re-planning of UAV/UGV search trajectories. Figure 4 presents a high-level overview of the proposed algorithm.

4.1 Phase 1: Search-Agent Trajectory Planning

Initial search planning is carried out (off-line) before the UAVs and UGVs are deployed in the field. One may note that the former is reliant on information obtained *a priori*. If this information were to be significantly different from the reality observed, a re-planning of the search would be required as soon as UAVs and UGVs are deployed in the field. The same is true for search-resource availability. If UAVs and UGVs that were expected to contribute to the search were unable to do so as expected, re-planning would be required upon determining the true capabilities of search resources.

4.1.1 UAV Search Planning

For UAVs, moving along a chosen single iso-probability curve with high speeds, for the entire duration of the search would lead to saturation of the search effort. Namely, a significant bias in the assignment of search effort would occur toward the selected percentile targets. In our method, thus, the UAVs search a range of iso-probability curves while spending an equal amount of search effort on each curve. Since iso-probability curves are, by definition, representative of equally likely target types (*i.e.*, targets of different propagation rate percentiles), searching all curves with equal effort translates to searching all target types with equal effort. This achieves the objective of optimal search outlined in Section 2.2. For a single UAV, the range of iso-probability curves to search is the entire set, 0% to 100%, of the iso-probability curves. Figure 5 shows a single UAV trajectory planned to search the complete set of iso-probability curves (0 to 100%).

For multiple UAVs, however, the range of iso-probability curves needs to be divided between them to achieve a more effective search. One way to achieve this division of work is to optimally partition the iso-probability curves between the UAVs in order to maximize the probability of target detection. Factors that influence this optimal division of work include UAV flight speed and starting location. The former directly impacts the range of iso-probability curves that can be covered by a UAV within the allotted search time. Namely, a slower UAV would be allocated a smaller range of iso-probability curves to ensure it can cover all curves with an equal amount of effort. Starting locations can also influence the assignment of UAVs to iso-probability curve ranges in that a correct assignment can maximize the amount of time UAVs have to search. An optimal assignment of UAVs to iso-probability curve ranges will minimize the amount of time they take to reach the start of their assigned ranges.

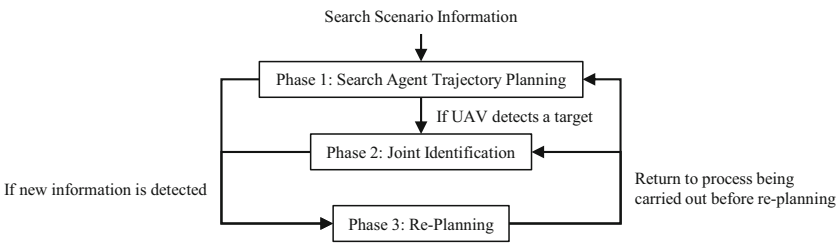

Fig. 4 The high-level algorithmic flow of the proposed method

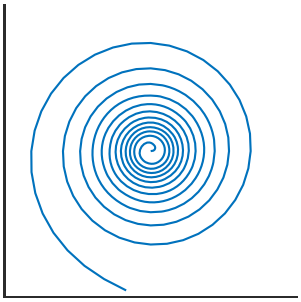

Fig. 5 An example UAV trajectory searching from the 0% to the 100% iso-probability curve

Other factors, such as battery level and distance to the target were not considered in this work or they were assumed to not affect search planning. UAV battery capacity, for example, was assumed to be large enough that UAVs do not require recharging during the search. Distance to the target could not be considered as its location is assumed to be unknown throughout the search.

Figure 6 shows a set of three UAV search trajectories, respectively, all starting at the LKP of the target [0,0]. In this example, the three UAVs search between the (*a*) 0%-51%, (*b*) 51-71%, and (*c*) 71%-100% iso-probability curves, respectively.

Trajectory Planning for A Single UAV The effort expended searching for the target, on a given curve, can be expressed as the proportion of possible targets that the UAV considers on the curve. Since it is assumed that the target may move away from the LKP in any direction, the range of angular positions considered on a curve is equal to the proportion of possible target motions of the corresponding percentile searched by the UAV. By the transitive property, then, the effort expended on a curve is proportional to the range of angular positions traversed on a curve:

$$\delta E(t) \propto \delta\theta(t). \tag{9}$$

For equal effort allocation, then, the UAV should traverse iso-probability curve percentiles at a rate proportional to its angular velocity. Incrementally, when a UAV is travelling from the $P_0\%$ iso-probability curve to the $P_0 + \delta P\%$ curve, it will proportionally traverse an angular position range of θ_0 to $\theta_0 + \delta\theta$, where:

$$\delta P = C\delta\theta. \tag{10}$$

Above, C is a proportionality constant. It is determined such that the UAV reaches the end of its overall allocated range of iso-probability curves at the end of the search, t_{end}.

UAV trajectory planning requires optimizing the incremental time unit, δt, to intercept the $P_0 + \delta P\%$ iso-probability curve at angular position $\theta_0 + \delta\theta$. Let us assume that at time t_0 the UAV is located at $\mathbf{x}_a(t_0) = [x_a(t_0), y_a(t_0)]^\top$ and angular position $\theta_0 = \text{atan}(y_a(t_0)/x_a(t_0))$. As the next step, it should reach/intercept the $P_0 + \delta P\%$ curve at $\theta_0 + \delta\theta$, Fig. 7. Since the destination and origin points are known (though mobile), it suffices to determine δt such that the distance the UAV travels during this incremental time is equal to the distance between the destination at time $t_0 + \delta t$ and the UAV's origin:

$$\delta t||\mathbf{v}_a|| = ||\mathbf{d}_{ac}(\theta_0 + \delta\theta, t_0, \delta t, P_0 + \delta P)||. \tag{11}$$

Above, $\mathbf{v}_a$ is the UAV's velocity and $\mathbf{d}_{ac}(\theta, t_0, \delta t, P)$ is the distance between the destination (at angular position θ on the $P\%$ iso-probability curve at time $t_0 + \delta t$) and the UAV origin, $\mathbf{x}_a(t_0)$:

$$d_{ac}(\theta, t_0, \delta t, P) = \mathbf{x}_c(\theta, t_0 + \delta t, P) - \mathbf{x}_a(t_0), \tag{12}$$

where $\mathbf{x}_c(\theta, t, p) = [x_c(\theta, t, p), y_c(\theta, t, p)]^\top$, defines the $p\%$ iso-probability curve at time t as a function of angular direction θ. The solution for positive δt is taken and used to compute the UAV's next position and heading. One may note that (12) assumes a linear trajectory between end points. Other methods, such as the one described in [53], could be used to quickly plan a smooth trajectory between end points, if required. Furthermore, when solving for δt, the UAV speed, $||\mathbf{v}_a||$, is assumed to be constant. Namely, it is assumed that UAVs always move at their maximum speed, which is maintained to maximize the UAV's coverage of the search area.

As will be further detailed below, for cooperative teams of UAVs and UGVs, while the UAVs search ranges of iso-probability curves, UGVs are assigned to individual iso-probability curves due to their slower speeds. Thus, herein,

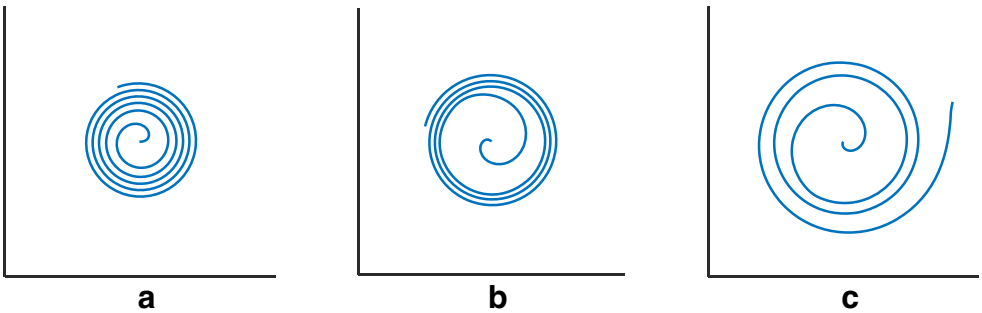

Fig. 6 A set of three UAV trajectories planned to collectively search for the mobile target. The UAVs are each searching the **a** 0%-51%, **b** 51-71%, and **c** 71%-100% iso-probability curve ranges, respectively

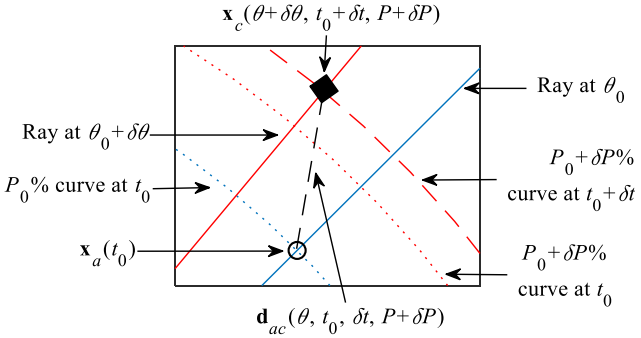

Fig. 7 The interception problem in UAV trajectory planning

UAV trajectory planning considers the search by the UGVs (*i.e.*, coordinated motion planning). Namely, when in the vicinity of an UGV-searched iso-probability curve, the UAV skips over this curve.

Pseudo-Redundant Coverage In UAV trajectory planning, pseudo-redundant coverage can be avoided by constraining the outwards propagation of the UAV [45]. For a single UAV moving along a single (static) iso-probability curve, one possible approach is to create a time-phased offset, perpendicular to the curve, so that, by the time the UAV makes a full circle, its coverage area no longer overlaps with the confidence area. The offset required to avoid pseudo-redundant coverage is defined as:

$$d_{\perp\min} = \left(r_a - v_{t\max} l/\|\mathbf{v}_a\|\right) + r_a, \tag{13}$$

where r_a is the UAV detection radius, l is the length of the curve, and $v_{t\max}$ is the target's maximum possible speed. The first term in (13) is the radius of the confidence area at the original location. The confidence area diminishes at a rate of $v_{t\max}$ and it takes the UAV $l/\|\mathbf{v}_a\|$ to traverse the entire iso-probability curve. The minimum outwards velocity required to avoid pseudo-redundant coverage is, then,

$$v_{\perp\min} = d_{\perp\min}/(l/v_u) = 2r_u v_u/l - v_{t\max}. \tag{14}$$

For a UAV that searches through a range of (propagating) iso-probability curves, a check is performed after solving (11) to determine the UAV's next heading. If the component of the UAV's velocity perpendicular to the curve is less than $v_{\perp\min}$, the heading is adjusted. Namely, the UAV's heading is changed such that the perpendicular component of the UAV's velocity is equal to $v_{\perp\min}$. The UAV, then, holds this new heading until it reaches an angular position of $\theta_0 + \delta\theta$, after which, planning resumes as normal.

4.1.2 UGV Search Planning

Three sub-problems need to be addressed for multi-UGV search planning [46, 54]. First, the number of iso-probability curves and their percentiles need to be selected to minimize a weighted sum of search-time, T_n, return-time, E_n, and success-rate, S_n, metrics:

$$\text{minimize}\, B = w_T(0.5T_n + 0.5E_n) + w_S S_n, \tag{15}$$

where w_T is the weighting for a combined search-time and return-time metric and w_S is the weighting of the success-rate metric. Second, during the selection, if the number of UGVs were to exceed the optimal number of curves, the UGV-to-iso-probability-curve assignment problem would need to be solved for equal effort and equal coverage. This can be achieved by assigning a number of UGVs proportional to the length of the curve:

$$n_{gj} = \lfloor n_g l_j / l_{total} + 0.5 \rfloor, \tag{16}$$

where n_{gj} is the number of UGVs assigned to the j^{th} curve, n_g is the total number of UGVs, l_j is the length of the j^{th} curve, and l_{total} is the total length of all curves (*i.e.*, $l_{total} = \sum_j l_j$). The third problem at hand is individual UGV trajectory planning. For this problem, one must note that, once assigned to its respective curve, a UGV must stay on it throughout the search, as the curve propagates outward from the LKP, Fig. 2 above. Only this third problem is detailed herein.

Trajectories that keep UGVs on their respective propagating iso-probability curves are planned incrementally, assuming the UGV always moves at its fastest pace. At each time step, the relevant iso-probability curve is propagated forward to the next time step and a motion direction is chosen for the UGV such that it ends up on the propagated curve at the next time step.

Let us consider a UGV at $\mathbf{x}_g(t_0) = [x_g(t_0), y_g(t_0)]^\top$ at time t_0, assigned to search the $P\%$ iso-probability curve. The UGV's location at the next time-step, $t_0 + \delta t$, is, then,

$$\mathbf{x}_g(t_0 + \delta t) = \mathbf{x}_g(t_0) + \mathbf{v}_g\left(\mathbf{x}_g(t_0), \hat{\mathbf{v}}_g\right)\delta t, \tag{17}$$

where $\mathbf{v}_g$ is the UGV's velocity during the next time step and $\hat{\mathbf{v}}_g$ is the unit velocity vector. The UGV's current position defines the terrain it is traversing, while the UGV's direction of travel defines its orientation with respect to the terrain. Both factors affect the UGV's speed. For example, a UGV heading uphill would have a lower speed than a UGV heading downhill [55].

Let us suppose, now, that the iso-probability curve being searched is defined by $\mathbf{x}_c(\theta, t, p) = [x_c(\theta, t, p), y_c(\theta, t, p)]^\top$, where θ is the angular direction away from the LKP, t is the time during the search, and p is the percentile target associated with the curve. Planning the UGV's heading between t_0 and $t_0 + \delta t$ is, then, a one-dimensional problem of finding a point on the iso-probability curve at time $t_0 + \delta t$ that the UGV will

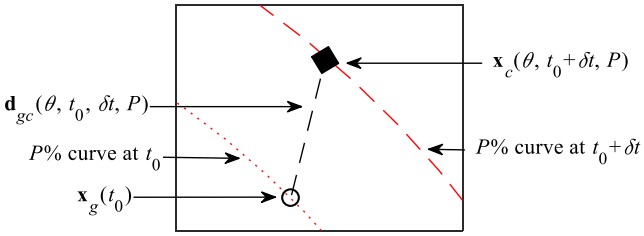

Fig. 8 The interception problem in UGV trajectory planning

arrive at just in time, Fig. 8. Mathematically, this can be expressed as finding a θ value such that,

$$\left|\left|\mathbf{v}_g\left(\mathbf{x}_g(t_0), \hat{\mathbf{d}}_{gc}(\theta, t_0, \delta t, P)\right)\right|\right| \delta t = \left|\left|\mathbf{d}_{gc}(\theta, t_0, \delta t, P)\right|\right|, \quad (18)$$

where $\mathbf{d}_{gc}(\theta, t_0, \delta t, P)$ is the distance between the destination (at θ on the iso-probability curve at time $t_0 + \delta t$) and the UGV origin, $\mathbf{x}_g(t_0)$:

$$\mathbf{d}_{gc}(\theta, t_0, \delta t, P) = \mathbf{x}_c(\theta, t_0 + \delta t, p) - \mathbf{x}_g(t_0), \quad (19)$$

and $\hat{\mathbf{d}}_{gc}(\theta, t_0, \delta t, P)$ is the unit vector in the direction of $\mathbf{d}_{gc}(\theta, t_0, \delta t, P)$. One may note that a UGV's speed at any given time is dependent on its current position as well as its travel direction. Namely, its speed is varied based on terrain. Additionally, it is assumed that some regions of the search area may not be traversable by the UGVs (*e.g.*, ponds, cliffs, large boulders) and, consequently, their trajectories must be altered to go around them. In the proposed method, UGVs take the shortest path when going around obstacles and return to their assigned iso-probability curve as soon as possible.

The right hand side of (18) represents the distance the UGV must travel to get to the point $\mathbf{x}_c(\theta, t_0 + \delta t, p)$, while the left hand side represents the distance the UGV would travel if it were to move towards $\mathbf{x}_c(\theta, t_0 + \delta t, p)$ for an interval of Δt. Determining a θ value, to solve (18), is equivalent to finding a point on the destination iso-probability curve at which the UGV would arrive at the same time as would the iso-probability curve. The sequence of such points approximates the trajectory the UGV must follow to stay on its respective iso-probability curve as it is propagating outward.

The above trajectory-planning procedure is carried out for all UGVs to define their respective search trajectories to follow for the duration of the search. Figure 9 shows a set of six UGV search trajectories assigned to search the (*a*) 10%, (*b*) 50%, and (*c*) 90% iso-probability curves. In this case, one UGV is assigned to the 10% curve, two UGVs are assigned to the 50% curve, and three UGVs are assigned to the 90% curve, Fig. 4a, b, c, respectively.

One may note that, when solving (18), two solutions would be found in most cases. In order to resolve this, a direction of motion is initially defined for the UGVs (*i.e.*, counter clockwise) and the closest point in that direction is taken to be the desired solution.

4.2 Phase 2: Joint Identification

As previously mentioned, it is assumed that UAVs rely on UGVs to identify a target that they detect. Thus, when a UAV discovers a target, it enters a *tracking mode* to maintain a visual of the target until a dispatched UGV reaches/intercepts it [56, 57]. Joint identification is, thus, a three-step process. First, a UAV detects a target and tracks it. Next, a UGV is dispatched to intercept this target. Lastly, if the target identified is the one sought, the search ends; otherwise, both the UAV and UGV must resume their respective search.

4.2.1 UGV Interception

As noted above, when a target is detected by a UAV, it is continually tracked and its estimated global position and velocity, $(\mathbf{x}_t(t), \dot{\mathbf{x}}_t(t))$, transferred in real-time to the designated interceptor (*i.e.*, the 'closest' UGV) with position and velocity $(\mathbf{x}_g(t), \dot{\mathbf{x}}_g(t))$. Given the current UGV and target positions at the current time, t_0, the objective of the subsequent target interception is to minimize the time span, δt, to target interception, (*i.e.*, when UGV and target positions coincide):

$$\mathbf{x}_g(t_0 + \delta t) = \mathbf{x}_t(t_0 + \delta t). \quad (20)$$

Interception can be carried out using a variety of guidance methods. One approach is following the parallel navigation guidance rule, which results in minimum-time interception if the target moves with a constant velocity, Fig. 10 [58, 59].

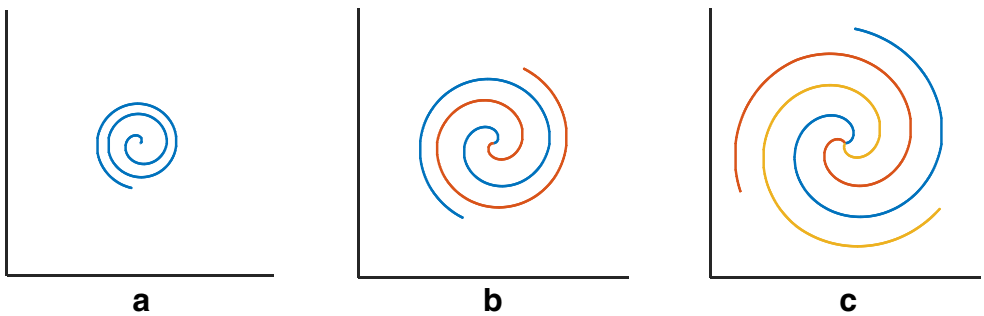

Fig. 9 An example set of six (different-colored) UGV search trajectories searching the **a** 10% (one UGV), **b** 50% (two UGVs), and **c** 90% (three UGVs) iso-probability curves as they propagate outward with time

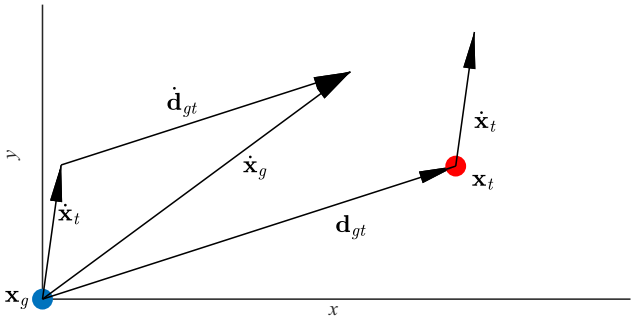

Fig. 10 The geometry of the parallel navigation rule

This approach begins by defining a line of sight (LOS), the relative position of the target with respect to the UGV:

$$\mathbf{d}_{gt} = \mathbf{x}_t - \mathbf{x}_g. \tag{21}$$

Similarly, the relative velocity of the target with respect to the UGV is defined by considering the time-derivative of (21):

$$\dot{\mathbf{d}}_{gt} = \dot{\mathbf{x}}_t - \dot{\mathbf{x}}_g. \tag{22}$$

The parallel-navigation rule stipulates that the relative velocity between the target and UGV should be antiparallel to the LOS. Following this rule results in the relative distance $\mathbf{d}_{gt}$ decreasing until 'collision'.

Given a known target velocity, $\dot{\mathbf{x}}_t$, it is possible to derive an expression for the UGV velocity required for interception. The derivation begins by formalizing the parallel-navigation law as a pair of equations:

$$\mathbf{d}_{gt} \times \dot{\mathbf{d}}_{gt} = 0, \tag{23}$$

$$\mathbf{d}_{gt} \cdot \dot{\mathbf{d}}_{gt} < 0, \tag{24}$$

Where "×" in (23) is the vector cross product. Above, (23) requires the LOS and relative velocity vectors to be parallel, while (24) specifies that the two vectors should point in opposite directions. Namely, the two equations specify that $\mathbf{d}_{gt}$ and $\dot{\mathbf{d}}_{gt}$ should be antiparallel. This set of equations can be solved to obtain that:

$$\dot{\mathbf{d}}_{gt} = -\alpha \mathbf{d}_{gt}, \tag{25}$$

where α is some positive constant. Combining this result with (22) and solving for the UGV velocity,

$$\dot{\mathbf{x}}_g = \dot{\mathbf{x}}_t + \alpha \mathbf{d}_{gt}. \tag{26}$$

The value of α can be determined by ensuring that the magnitude of $\dot{\mathbf{x}}_g$ is equal to the maximum UGV velocity. In complex environments with moving obstacles, the methods presented in [60, 61] can be used to address the interception problem as it expands upon the parallel navigation guidance rule, using a velocity-obstacle approach for obstacle avoidance.

4.2.2 Loss of Tracking

Due to the UAV's inability to 'see' through dense tree-coverage, it is possible that it might lose sight of the originally detected target before a UGV has a chance to intercept it. In such a case, the target's motion characteristics are estimated and used to extrapolate future target motion. Namely, a *virtual target* that follows the same (expected) trajectory of the original one is generated and tracked by the UAV while the UGV continues to move toward it.

While the exact method used will depend on the target model at hand, characteristic estimation can be performed in a variety of ways [62, 63]. For the model used herein, for example, methods such as maximum likelihood estimation (MLE) could be used to estimate the parameters $d_{\max}$ and σ_θ in the probabilistic motion model given target motion observed after the UAV encounters the target [63]. Namely, given n observations of the distance travelled, $D = \{d_1, \cdots, d_n\}$, and m, observations of directions taken, $\Theta = \{\theta_1, \cdots, \theta_m\}$, estimates d_{MLE} and σ_{MLE} could be determined by optimizing them to maximize the average log-likelihood of the observed data:

$$\hat{l}(d_{\text{MLE}}; D) = \frac{1}{n}\sum_{i=1}^{n} \ln(f_d(d_i, d_{\text{MLE}})), \tag{27}$$

$$\hat{l}(\sigma_{\text{MLE}}; \Theta) = \frac{1}{m}\sum_{i=1}^{m} \ln(f_\theta(\theta_i, \sigma_{\text{MLE}})). \tag{28}$$

Above, $f_d(d_i, d_{\text{MLE}})$ is the likelihood of datum d_i given the parameter d_{MLE} and $f_\theta(\theta_i, \sigma_{\text{MLE}})$ is the likelihood of datum θ_i given the parameter σ_{MLE}. Similarly, estimators like those that build on the extended Kalman filter (EKF) could be used to estimate the mean target walking speed given observations of noisy and terrain-affected walking speeds [64].

If the original target emerges from tree cover, near its expected exit location, it is re-detected by the UAV and its tracking resumes. Otherwise, if the target does not emerge from tree cover when and where expected, the planned interception is aborted and both the UAV and UGV return to their respective searches.

4.2.3 Post-Interception

As noted above, if the target intercepted by the UGV is a *false positive*, both the tracking UAV and the intercepting UGV must return to their respective searches. In the UAV's case, since it has expended time tracking the target, it cannot resume its original trajectory from where it left off. Namely, since its initial search trajectory was planned such that it would arrive at its final iso-probability curve at the end of the search, *just-*

in-time, any detours would result in a late arrival at the final iso-probability curve. Thus, the UAV must have its entire search trajectory re-planned such that it resumes search on the iso-probability curve it left off and completes a search of the remaining iso-probability curve range.

The UAV trajectory re-planning process is identical to that of the initial planning phase with modified inputs. Namely, the new objective would be to plan a search trajectory such that the UAV (now) starts its search on the (new) starting iso-probability curve and ends on the (original) ending iso-probability curve at the end of search time.

In the UGV's case, this simply implies the vehicle returning to its designated iso-probability curve as soon as possible. The fastest path to its designated curve could be determined by using a shortest-path finding algorithm. One example is the A* search algorithm, which could be run on a graph defined over the search space with edges weighted with terrain-influenced travel times.

4.3 Phase 3: Re-Planning

While target-motion uncertainty is explicitly considered in search planning (*i.e.*, plans are made based on a probabilistic target location estimate), other uncertainties are handled through search re-planning. When significant information regarding the target's whereabouts is discovered (*e.g.*, a clue), the current search can be considered sub-optimal unless re-planned. In such a case, our method requires all searchers (except those involved in a potential interception) halt their current search and re-start on newly re-planned search trajectories.

For UAVs, the search planning process is re-executed in its entirety. Namely, UAV trajectories are re-planned such that they collectively search the entire range of iso-probability curves with equal effort in the remaining search time.

Furthermore, re-planning is different from the original planning in that UAV assignments to ranges of iso-probability curves needs to be optimized. Since UAVs halt mid-search, they are no longer all at the LKP and will take different amounts of time to reach the start of their assigned range. UAVs assignments to their percentile ranges are carried out such that the maximum time spent reaching their assigned range is minimized. A similar problem, the linear bottleneck assignment problem, was addressed in [54] and solved with the Threshold algorithm.

For UGVs, search planning is re-executed from the start as well. This includes iso-probability curve selection, UGV-curve assignment, and trajectory planning. During curve selection and UGV-curve assignment, re-planning additionally considers how long it will take the robots to reach their next curves. Namely, since UGVs are scattered throughout the search area, they will reach their new assigned iso-probability curves at different times. Thus, as in the UAV re-planning case, they must be assigned to curves such that travel time is minimize [54].

5 Illustrative and Comparative Simulations

In this Section, a set of three illustrative examples, showing different scenarios of target detection, is presented first. Results of numerous comparative studies to other methods, as well as a short discussion, are then discussed.

5.1 Illustrative Examples

The proposed method is demonstrated herein through three example searches. In all examples, a team of ten UGVs (blue dots in the figures), with a max speed of 10 m/s and a detection radius of 5 m, and three UAVs (green dots in the figures), with a max speed of 100 m/s and a (ground) detection radius of 30 m, search for a lost target in the wilderness. The search area comprises a variable terrain with elevation (color gradient), tree coverage (gray circles), and impassible obstacles (black blobs), Fig. 11. In all cases, the search starts 8000 s after the target has left the LKP and is planned to last for an additional 3000 s, until 11,000 s. All UAVs and UGVs start their motion at the LKP.

In all cases, the three UAVs search the (optimally determined) 0 to 48%, 48 to 78%, and 78 to 100% iso-probability curve ranges, respectively. The UGVs remain on the 10%, 30%, 50%, 70%, and 90% iso-probability curves, with a distribution of (1, 2, 2, 2, 3) vehicles, respectively.

All searches are planned assuming the target's walking speed is normally distributed with a mean of $\mu = 0.5$ m/s and a standard deviation of $\sigma = 0.166$ m/s. Furthermore, the target motion model is assumed to have a '*wandering*' parameter of $\sigma_\theta = \pi/3$ rad and a '*decisiveness*' parameter of $d_{\max} = 100$ m. All examples contain one 'true' target and one 'false' target (red dot and a pink cross, respectively). Both targets start their motion at (0,0).

5.1.1 Example 1

In this example, the initially located and tracked target by a UAV is the 'true' one, as identified by the UGV that intercepts it.

Figure 12 shows four snapshots of the search. For simplicity, each snapshot shows the paths taken by the search agents only for the previous 30 s, and the entire path taken by the target since $t = 0$ s (red and pink for the true and false targets respectively).

At 8000 s, Fig. 12a, all search units leave the LKP, $(x, y) = (0,0)$, and begin their search. At 9000 s, Fig. 12b, all UAVs and UGVs have been travelling along their respective iso-probability curve ranges and curves for some time. Their

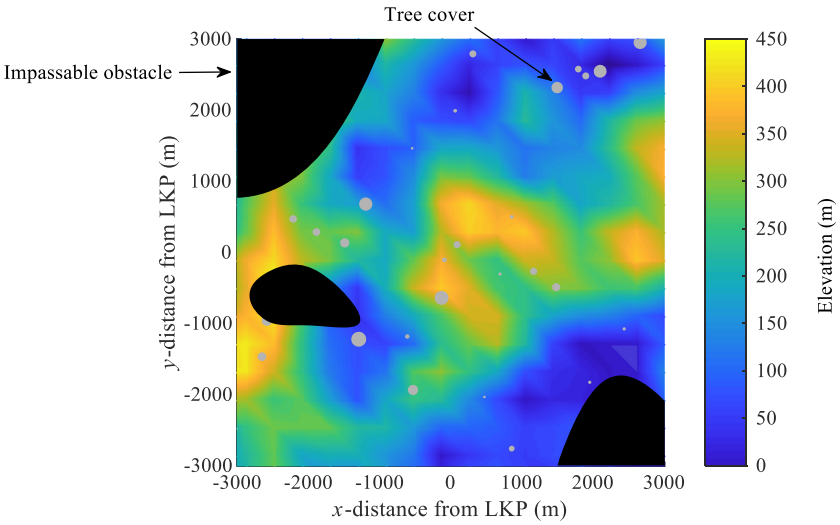

Fig. 11 Terrain for Searches in Examples 1 to 3

past paths on these curves are illustrated by solid lines. At 10,231 s, Fig. 12c, UAV-1, searching the 0 to 48% iso-probability curve range, locates a target at $(x, y) = (-774, -1113)$. Subsequently, the nearest ground vehicle, UGV-5, moving on the 50% iso-probability curve, is dispatched to intercept the target. Figure 12d is a close-up illustration, at 10,285 s, where the target is intercepted by UGV-5 at $(x, y) = (-781, -1104)$ and identified as the ('true') one searched.

5.1.2 Example 2

In this example, first, the 'false' target is located by a UAV, as later determined by the UGV that intercepts it. The 'true' target is located later by a different UAV, as verified by the UGV that intercepts it.

Figure 13 shows four snapshots of the search. The initial configuration at 8000 s is omitted for brevity. At 8761 s,

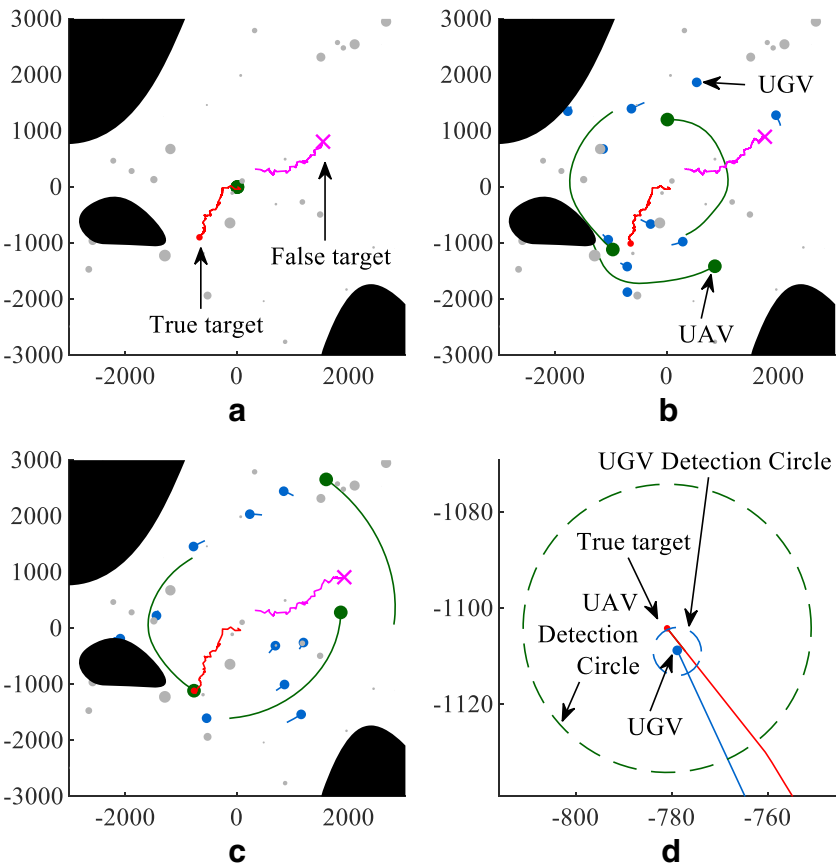

Fig. 12 Example 1: Search at **a** 8000 s, **b** 9000 s, **c** 10,231 s, and **d** 10,286 s. True target trajectory (red); false target trajectory (pink); UAV trajectory (green); and, UGV trajectory (blue)

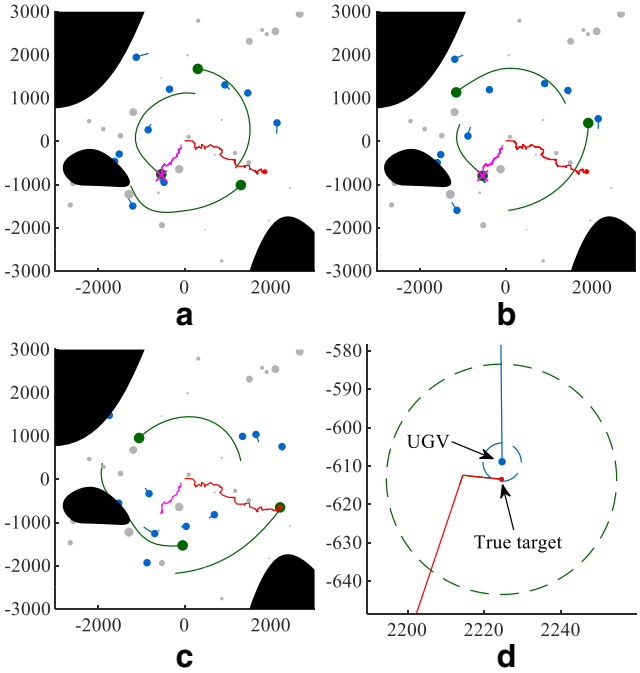

Fig. 13 Example 2: Search at **a** 8761 s, **b** 8777 s, **c** 9857 s, and **d** 9993 s. True target trajectory (red); false target trajectory (pink); UAV trajectory (green); and, UGV trajectory (blue)

Fig. 13a, UAV-1, searching the 0 to 48% iso-probability curve range, locates a target at $(x, y) = (-546, -796)$. The nearby UGV-2, searching the 30% iso-probability curve, is dispatched to intercept it. At 8777 s, Fig. 13b, the target is intercepted, but determined to be not the one searched. Consequently, both UAV-1 and UGV-3 return to their original searches. At 9857 s, Fig. 13c, UAV-3, searching the 78 to 100% iso-probability curve range, locates another target and the nearby UGV-10, searching the 90% iso-probability curve, is dispatched to intercept it. Figure 13d is a close-up illustration, at 9993 s, where the target is intercepted by UGV-10 at $(x, y) = (2224, -613)$ and identified as the ('true') one searched. A video illustrating Example 2 can be found at [65].

5.1.3 Example 3

In this example, a target is detected by a UAV, but, then, lost to tree cover, re-discovered, and finally intercepted.

Figure 14 shows three snapshots of the search, with corresponding close-ups. At 9104 s, Fig. 14a, UAV-3, searching the 78 to 100% iso-probability curve range, locates a target at $(x, y) = (-1277, -1329)$. The nearby UGV-7, searching the 70% iso-probability curve, is dispatched to intercept it. However, before UGV-7 has a chance to intercept the target, UAV-3 loses it to tree cover.

UAV-3 continues to track the virtual target (*i.e.*, the target's predicted location), based on its last known velocity. However, when the UGV arrives at the predicted (virtual) target location at 9186 s, it detects no target, Fig. 14b. The

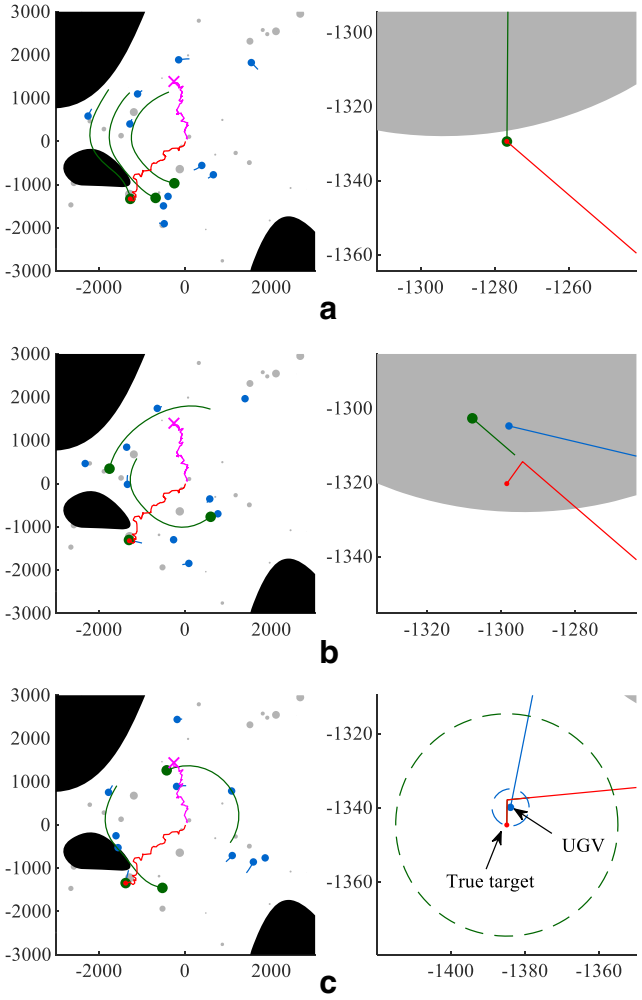

Fig. 14 Snapshots of the search described in Example 3 at **a** 9104 s, **b** 9186 s, and **c** 9523 s. True target trajectory (red); false target trajectory (pink); UAV trajectory (green); and, UGV trajectory (blue)

target had changed direction while under tree cover. With the target lost, both UAV-3 and UGV-7 return to their original searches.

At 9433 s, another target is located by UAV-3. The nearby UGV-2, searching the 30% iso-probability curve, is dispatched to intercept it. Figure 14c shows the interception, at 9, 523 s, by UGV-2 at $(x, y) = (-1385, -1345)$ and identified as the ('true') one searched.

5.2 Comparative Simulations

In order to further validate the effectiveness and efficiency of the proposed collaborative search-planning method, comparative simulated search experiments were performed against two alternative methods: a pattern-based search [66], which is typical in traditional WiSAR, and a method addressing the target localization in outdoor environments [38], a problem similar to the one considered here. The latter method addresses the problem by using an on-line search-planning

controller that maximizes the information acquired with each motion. One may note that the successful validation of this work was limited to simulated search experiments, though, reflecting as closely as possible real-world performance. Namely, the results of the simulations provide valuable insight into conditions under which the proposed method would perform better than other existing methods.

For the first alternative method, AM-1, both the UAVs and the UGVs start their motion at the LKP and follow Archimedean spiral search trajectories, which approximate uniform coverage of the search area, [66], Fig. 15. For multi-UAV teams, the search area is partitioned into concentric regions, where each is searched by a single UAV, as per our proposed method. Partitions are optimized such that all UAVs finish their search at the same time and all regions are *covered* equally. UGVs also follow Archimedean spirals outward from the LKP to the outer edge of the search area. Their spirals are offset such that redundant coverage is minimized.

The second alternative method, AM-2, considered herein was originally developed for static targets, where UAVs obtain initial estimates of target locations and, subsequently, UGVs refine these estimates [38], Fig. 16. For a fair comparison, this method was modified to be applicable to mobile targets. Modifications included: (*i*) avoidance of pseudo-redundant coverage during UAV and UGV motion planning, and (*ii*) having the UAVs continue to track the mobile targets until a UGV confirms their identity.

Both alternative methods were compared to our proposed method in terms of their target detection performance as well as UGV responsiveness, using 1000 randomly sampled targets. For the latter metric, the time required by a UGV to intercept the target was examined. A faster interception time would be indicative of a more responsive cooperation between the UGVs and UAVs. Two sets of representative experimental results are presented herein.

For the first set of experiments, the search team comprised one UAV, capable of moving at a speed of up to 50 m/s, and 15 identical UGVs, capable of moving at speeds of up to 5 m/s, respectively. All searches started 3600 s after the target has left the LKP, and continued for another 3600 s (*i.e.*, a total of 7200 s). The target demographic had normally distributed

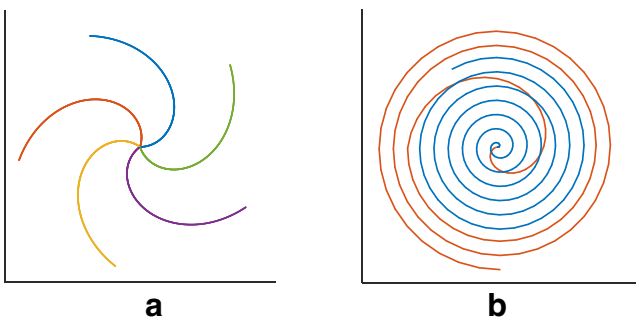

Fig. 15 Example AM-1 search trajectories for **a** 5 UGVs and **b** 2 UAVs

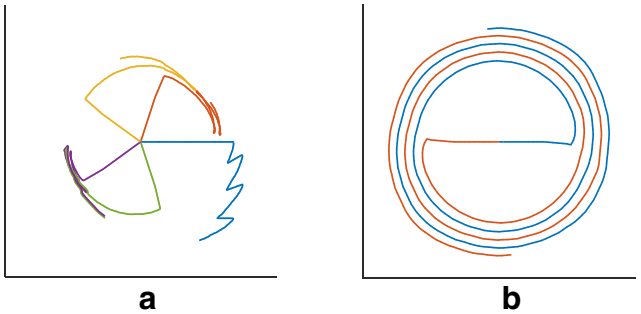

Fig. 16 Example AM-2 search trajectories for **a** 5 UGVs and **b** 2 UAVs

walking speeds with a mean of 0.7 m/s and a standard deviation of 0.23 m/s and random motion model parameters of $d_{max} = 100$ and $\sigma_\theta = \pi/3$.

Table 1 below shows (*a*) the number of targets detected by UAVs that are, subsequently, intercepted by UGVs, (*i.e.*, *UAV→UGV)*, as well as (*b*) the number of targets detected/intercepted (only) by UGVs without the help of a UAV. For the former case, (*i.e.*, *UAV→UGV)*, the results indicate that the proposed method performs tangibly better than do both alternative methods, on average by about 170% over AM-1 and 190% over AM-2, respectively. For the overall case (*i.e.*, *Total = UAV→UGV + UGV only)*, the results validate that the proposed method can still perform tangibly better than do both alternative methods, on average by about 130% over AM-1 and 180% over AM-2, respectively.

As expected, it was noted that, the AM-1 distributes its search effort across the whole search area, but in a suboptimal manner, resulting in a higher detection rate than AM-2's but lower than the proposed method's. Also, as expected, the UAV contribution to the search, typically, decreases with increasing UGV detection radius. This is due to the UGVs locating targets earlier than they would have been found by the UAVs.

Mean target interception times by the UGVs after a UAV-detection (i.e., *UAV→UGV)*, as noted in Table 1 above, are shown in Table 2 below. The results indicate that the responsiveness of the UGVs is (statistically) comparable for all three methods.

For the second set of experiments, the search team comprised three identical UAVs and 15 identical UGV, with the same characteristics as for the first set of experiments.

Table 1 Number of target detections for one UAV and 15 UGVs

Proposed Method / AM-1 / AM-2			
$r_{UAV} - r_{UGV}$ *(m – m)*	30 – 5	30 – 15	30 – 30
UAV→UGV	322 / 116 / 133	315 / 116 / 110	293 / 115 / 84
UGV only	77 / 38 / 12	165 / 96 / 57	294 / 174 / 133
Total	399 / 154 / 145	480 / 212 / 167	587 / 289 / 217

Table 2 Mean interception times for one UAV and 15 UGVs

Proposed Method / AM-1 / AM-2			
$r_{UAV} - r_{UGV}$ *(m – m)*	30 – 5	30 – 15	30 – 30
Mean Time (s)	93 / 102 / 99	93 / 102 / 124	91 / 103 / 128

Table 3 below shows (*a*) the number of targets detected by UAVs that are, subsequently, intercepted by UGVs, (*i.e.*, *UAV→UGV)*, as well as (*b*) the number of targets detected/intercepted (only) by UGVs without the help of a UAV. For the former case, (*i.e.*, *UAV→UGV)*, the results indicate that the proposed method performs tangibly better than do both alternative methods, on average by about 90% over AM-1 and 345% over AM-2, respectively. For the overall case (*i.e.*, *Total = UAV→UGV + UGV only)*, the results validate that the proposed method can still perform tangibly better than do both alternative methods, on average by about 75% over AM-1 and 255% over AM-2, respectively.

The performance gap between the proposed method and AM-1 is somewhat reduced with additional UAVs, from about 130% improvement to about 75%. This is expected since AM-1 is a form of uniform coverage search and, given enough UAVs, it will eventually find all targets.

Despite the greater search effort available, however, AM-2 still continues to focus its search where the target location likelihood is maximum, resulting in only slightly improved performance. Thus, the results clearly suggest that a larger number of UAVs accentuates the performance difference between the proposed method and AM-2.

Mean target interception times by the UGVs after a UAV-detection (*i.e.*, *UAV→UGV)*, as noted in Table 3 above, are shown in Table 4 below. The results indicate that AM-1 performs significantly worse in terms of interception time. This is due to UAVs being quickly distributed between the three partitions while UGVs search and progress outwards from the LKP together. This contrasts with the one UAV case, where the UAVs and UGVs progress outwards nearly at the same rate. As a result, distances between UAVs and closest UGVs are, frequently, larger at detection instances, leading to higher interception times. The results, however, indicate that the responsiveness of the UGVs is (statistically) comparable between the proposed method and AM-2.

Table 3 Number of target detections for three UAVs and 15 UGVs

Proposed Method / AM-1 / AM-2			
$r_{UAV} - r_{UGV}$ *(m – m)*	30 – 5	30 – 15	30 – 30
UAV→UGV	650 / 341 / 140	618 / 328 / 132	571 / 309 / 143
UGV only	57 / 38 / 23	124 / 100 / 73	228 / 183 / 158
Total	707 / 379 / 163	742 / 428 / 205	799 / 492 / 301

Table 4 Mean interception times for 3 UAVs and 15 UGVs

Proposed Method / AM-1 / AM-2			
$r_{UAV} - r_{UGV}$ *(m - m)*	30 – 5	30 – 15	30 – 30
Mean Time (s)	136 / 206 / 165	138 / 207 / 142	139 / 208 / 133

6 Conclusions

In this paper, a novel mobile-target search-planning method is presented for collaborative UAV/UGV teams. The proposed method utilizes target iso-probability curves to plan both UAV and UGV trajectories. For UAVs, the proposed novel search-planning algorithm determines trajectories that traverse a range of iso-probability curves while covering them all with equal effort. Such a search achieves a balance between exploitation and exploration. The proposed method is further novel in that it allows for coordinated search and joint identification of lost targets. Namely, for targets that are first detected by a UAV, a UGV is employed to confirm identity.

Numerous simulated experiments were presented to illustrate and validate the proposed search-coordination and target-identification method. Comparative experiments showed that our method performs tangibly better than several alternative methods for WiSAR. It was shown to have a higher rate of target detection, as well as shorter search times in cases where the target is first detected by a UAV. In the best case, on average, the proposed method performed about 250% better than the alternative. Other methods, against which the proposed method was compared, performed comparably to the proposed method only when the search was started early. Namely, when the target had not propagated far from the LKP.

Acknowledgements The authors would like to acknowledge the support received, in part, by the Natural Sciences and Engineering Research Council of Canada (NSERC).

References

1. Navia, J., Mondragon, I., Patino, D., Colorado, J.: Multispectral Mapping in Agriculture: Terrain Mosaic Using an Autonomous Quadcopter UAV. In: Proc. Int. Conf. Unmanned Aircraft Syst. pp. 1351–1358, Arlington (2016)
2. Zhang, G., Shang, B., Chen, Y., Moyes, H.: SmartCaveDrone: 3D Cave Mapping Using UAVs as Robotic Co-Archaeologists. In: Proc. Int. Conf. Unmanned Aircraft Syst. pp. 1052–1057. Miami (2017)

3. Rasmussen, S., Kalyanam, K., Kingston, D.: Field Experiment of a Fully Autonomous Multiple UAV/UGS Intruder Detection and Monitoring System. In: Proc. Int. Conf. Unmanned Aircraft Syst. pp. 1293–1302., Arlington, VA, USA (2016)
4. Kang, D., Cha, Y.-J.: Autonomous UAVs for Structural Health Monitoring Using Deep Learning and an Ultrasonic Beacon System with Geo-Tagging. Comput.-Aided Civ. Infrastruct. Eng. **33**, 885–902 (2018). https://doi.org/10.1111/mice.12375
5. Leira, F.S., Johansen, T.A., Fossen, T.I.: A UAV Ice Tracking Framework for Autonomous Sea Ice Management. In: Proc. Int. Conf. Unmanned Aircraft Syst. pp. 581–590, Miami (2017)
6. Tripolitsiotis, A., Prokas, N., Kyritsis, S., Dollas, A., Papaefstathiou, I., Partsinevelos, P.: Dronesourcing: A Modular, Expandable Multi-Sensor UAV Platform for Combined. Real-Time Environmental Monitoring. Int. J. Remote Sens. **38**, 2757–2770 (2017). https://doi.org/10.1080/01431161.2017.1287975
7. Furukawa, T., Bourgault, F., Lavis, B., Durrant-Whyte, H.F.: Recursive Bayesian Search-and-Tracking Using Coordinated UAVs for Lost Targets. In: Proc. IEEE Int. Conf. Robot. Autom. pp. 2521–2526, Orlando (2006)
8. Ha, I.-K., Cho, Y.-Z., Ha, I.-K., Cho, Y.-Z.: A Probabilistic Target Search Algorithm Based on Hierarchical Collaboration for Improving Rapidity of Drones. Sensors. **18**, 2535 (2018). https://doi.org/10.3390/s18082535
9. Lin, L., Goodrich, M.A.: Hierarchical Heuristic Search Using a Gaussian Mixture Model for UAV Coverage Planning. IEEE Trans. Cybern. **44**, 2532–2544 (2014). https://doi.org/10.1109/TCYB.2014.2309898
10. Brown, D., Sun, L.: Exhaustive Mobile Target Search and Non-Intrusive Reconnaissance Using Cooperative Unmanned Aerial Vehicles. In: Proc. Int. Conf. Unmanned Aircraft Syst. pp. 1425–1431, Miami (2017)
11. Tang, Z., Ozguner, U.: On Non-Escape Search for a Moving Target by Multiple Mobile Sensor Agents. In: Proc. American Control Conf. pp. 3525–3530, Minneapolis (2006)
12. Hayat, S., Yanmaz, E., Brown, T.X., Bettstetter, C.: Multi-Objective UAV Path Planning for Search and Rescue. In: Proc. IEEE Int. Conf. Robot. Autom. pp. 5569–5574, Singapore (2017)
13. Pelosi, M., Brown, M.S.: Improved Search Paths for Camera-Equipped UAVS in Wilderness Search and Rescue. In: Proc. IEEE Symp. Series Comp. Intell. pp. 1–8, Honolulu (2017)
14. Sun, J., Li, B., Jiang, Y., Wen, C.: A Camera-Based Target Detection and Positioning UAV System for Search and Rescue (SAR) Purposes. Sensors. **16**, 1778 (2016). https://doi.org/10.3390/s16111778
15. Dinnbier, N.M., Thueux, Y., Savvaris, A., Tsourdos, A.: Target Detection Using Gaussian Mixture Models and Fourier Transforms for UAV Maritime Search and Rescue. In: Proc. Int. Conf. Unmanned Aircraft Syst. pp. 1418–1424, Miami (2017)
16. Goodrich, M.A., Morse, B.S., Gerhardt, D., Cooper, J.L., Quigley, M., Adams, J.A., Humphrey, C.: Supporting Wilderness Search and Rescue Using a Camera-Equipped Mini UAV. J. Field Robot. **25**, 89–110 (2008). https://doi.org/10.1002/rob.20226
17. Niedzielski, T., Jurecka, M., Miziński, B., Remisz, J., Ślopek, J., Spallek, W., Witek-Kasprzak, M., Kasprzak, Ł., Świerczyńska-Chlaściak, M.: A Real-Time Field Experiment on Search and Rescue Operations Assisted by Unmanned Aerial Vehicles. J. Field Robot. (2018). https://doi.org/10.1002/rob.21784
18. Tomic, T., Schmid, K., Lutz, P., Domel, A., Kassecker, M., Mair, E., Grixa, I.L., Ruess, F., Suppa, M., Burschka, D.: Toward a Fully Autonomous UAV: Research Platform for Indoor and Outdoor Urban Search and Rescue. IEEE Robot. Autom. Mag. **19**, 46–56 (2012). https://doi.org/10.1109/MRA.2012.2206473
19. Perez-Grau, F.J., Ragel, R., Caballero, F., Viguria, A., Ollero, A.: Semi-Autonomous Teleoperation of UAVs in Search and Rescue Scenarios. In: Proc. Int. Conf. Unmanned Aircraft Syst. pp. 1066–1074, Miami (2017)
20. Agcayazi, M.T., Cawi, E., Jurgenson, A., Ghassemi, P., Cook, G.: ResQuad: Toward a Semi-Autonomous Wilderness Search and Rescue Unmanned Aerial System. In: Proc. Int. Conf. Unmanned Aircraft Syst. pp. 898–904, Arlington, VA, USA (2016)
21. Duan, H., Liu, S.: Unmanned Air/Ground Vehicles Heterogeneous Cooperative Techniques: Current Status and Prospects. Sci. China Technol. Sci. **53**, 1349–1355 (2010). https://doi.org/10.1007/s11431-010-0122-4
22. Caska, S., Gayretli, A.: A Survey of UAV/UGV Collaborative Systems. In: Proc. Int. Conf. Comput. Ind. Eng. Int. Symp. Intell. Manufacturing Service Systs. Joint Int. Symp. "Social Impacts Developments Information Manufacturing Service Syst." pp. 453–463, Istanbul (2014)
23. Delmerico, J., Mueggler, E., Nitsch, J., Scaramuzza, D.: Active Autonomous Aerial Exploration for Ground Robot Path Planning. IEEE Robot. Autom. Lett. **2**, 664–671 (2017). https://doi.org/10.1109/LRA.2017.2651163
24. Reardon, C., Fink, J.: Air-Ground Robot Team Surveillance of Complex 3D Environments. In: Proc. IEEE Int. Symp. Safety, Security, Rescue Robot. pp. 320–327, Lausanne (2016)
25. Xiao, X., Dufek, J., Woodbury, T., Murphy, R.: UAV Assisted USV Visual Navigation for Marine Mass Casualty Incident Response. In: Proc. IEEE/RSJ Int. Conf. Intell. Robot. Syst. pp. 6105–6110, Vancouver (2017)
26. Christie, G., Shoemaker, A., Kochersberger, K., Tokekar, P., McLean, L., Leonessa, A.: Radiation Search Operations Using Scene Understanding With Autonomous UAV and UGV. J. Field Robot. **34**, 1450–1468 (2017). https://doi.org/10.1002/rob.21723
27. Marconi, L., Melchiorri, C., Beetz, M., Pangercic, D., Siegwart, R., Leutenegger, S., Carloni, R., Stramigioli, S., Bruyninckx, H., Doherty, P., Kleiner, A., Lippiello, V., Finzi, A., Siciliano, B., Sala, A., Tomatis, N.: The SHERPA Project: Smart Collaboration Between Humans and Ground-Aerial Robots for Improving Rescuing Activities in Alpine Environments. In: Proc. IEEE Int. Symp. Safety, Security, Rescue Robot. pp. 1–4, College Station (2012)
28. Qin, H., Meng, Z., Meng, W., Chen, X., Sun, H., Lin, F., Ang, M.H.: Autonomous Exploration and Mapping System Using Heterogeneous UAVs and UGVs in GPS-Denied Environments. IEEE Trans. Veh. Technol. **68**, 1339–1350 (2019). https://doi.org/10.1109/TVT.2018.2890416
29. Arbanas, B., Ivanovic, A., Car, M., Orsag, M., Petrovic, T., Bogdan, S.: Decentralized Planning and Control for UAV–UGV Cooperative Teams. Auton. Robot. (2018). https://doi.org/10.1007/s10514-018-9712-y
30. Li, J., Deng, G., Luo, C., Lin, Q., Yan, Q., Ming, Z.: A Hybrid Path Planning Method in Unmanned Air/Ground Vehicle (UAV/UGV) Cooperative Systems. IEEE Trans. Veh. Technol. **65**, 9585–9596 (2016). https://doi.org/10.1109/TVT.2016.2623666
31. Minaeian, S., Liu, J., Son, Y.-J.: Vision-Based Target Detection and Localization via a Team of Cooperative UAV and UGVs. IEEE Trans. Syst. Man Cybern. Syst. **46**, 1005–1016 (2016). https://doi.org/10.1109/TSMC.2015.2491878
32. Manyam, S.G., Casbeer, D.W., Sundar, K.: Path Planning for Cooperative Routing of Air-Ground Vehicles. In: Proc. American Control Conf. pp. 4630–4635, Boston (2016)
33. Tripathi, S.K., Sapre, R.M.: Robust Target Localization and Tracking Using Kalman Filtering for UGV-UAV Coordinated

Operation. In: Proc. Int. Conf. Recent Advances Innovations Eng. pp. 1–6. IEEE, Jaipur (2016)
34. Hood, S., Benson, K., Hamod, P., Madison, D., O'Kane, J.M., Rekleitis, I.: Bird's Eye View: Cooperative Exploration by UGV and UAV. In: Proc. Int. Conf. Unmanned Aircraft Syst. pp. 247–255. IEEE, Miami (2017)
35. Rosa, L., Cognetti, M., Nicastro, A., Alvarez, P., Oriolo, G.: Multi-task Cooperative Control in a Heterogeneous Ground-Air Robot Team. IFAC-Pap. **48**, 53–58 (2015). https://doi.org/10.1016/j.ifacol.2015.06.463
36. Lum, C.W., Vagners, J., Rysdyk, R.T.: Search Algorithm for Teams of Heterogeneous Agents With Coverage Guarantees. J. Aerosp. Comput. Inf. Commun. **7**, 1–31 (2010). https://doi.org/10.2514/1.44088
37. Sauter, J.A., Mathews, R.S., Yinger, A., Robinson, J.S., Moody, J., Riddle, S.: Distributed Pheromone-Based Swarming Control of Unmanned Air and Ground Vehicles for RSTA. In: Unmanned Systems Technology X. p. 69620C. International Society for Optics and Photonics (2008)
38. Grocholsky, B., Keller, J., Kumar, V., Pappas, G.: Cooperative Air and Ground Surveillance. IEEE Robot. Autom. Mag. **13**, 16–25 (2006). https://doi.org/10.1109/MRA.2006.1678135
39. Beck, Z., Teacy, L., Rogers, A., Jennings, N.R.: Online Planning for Collaborative Search and Rescue by Heterogeneous Robot Teams. In: Proc. Int. Conf. Autonomous Agents Multiagent Syst. pp. 1024–1033. International Foundation for Autonomous Agents and Multiagent Systems, Singapore (2016)
40. Pippin, C.E., Christensen, H.: A Bayesian Formulation for Auction-Based Task Allocation in Heterogeneous Multi-Agent Teams. In: Proc. Ground/Air Multisensor Interoperability, Integration, Networking Persistent ISR II. p. 804710. International Society for Optics and Photonics, Orlando (2011)
41. Fregene, K., Kennedy, D.C., Wang, D.W.L.: Toward a Systems-and Control-Oriented Agent Framework. IEEE Trans. Syst. Man Cybern. Part B Cybern. **35**, 999–1012 (2005). https://doi.org/10.1109/TSMCB.2005.848491
42. Flushing, E.F., Kudelski, M., Gambardella, L.M., Caro, G.A.D.: Connectivity-Aware Planning of Search and Rescue Missions. In: Proc. IEEE Int. Symp. Safety, Security, Rescue Robot. pp. 1–8, Linkoping (2013)
43. Yu, H., Meier, K., Argyle, M., Beard, R.W.: Cooperative Path Planning for Target Tracking in Urban Environments Using Unmanned Air and Ground Vehicles. IEEEASME Trans. Mechatron. **20**, 541–552 (2015). https://doi.org/10.1109/TMECH.2014.2301459
44. Macwan, A., Nejat, G., Benhabib, B.: Target-Motion Prediction for Robotic Search and Rescue in Wilderness Environments. IEEE Trans. Syst. Man Cybern. Part B Cybern. **41**, 1287–1298 (2011). https://doi.org/10.1109/TSMCB.2011.2132716
45. Kashino, Z., Nejat, G., Benhabib, B.: Multi-UAV based Autonomous Wilderness Search and Rescue using Target Iso-Probability Curves. In: Proc. Int. Conf. Unmanned Aircraft Syst. pp. 628–635, Atlanta (2019)
46. Macwan, A., Vilela, J., Nejat, G., Benhabib, B.: A Multirobot Path-Planning Strategy for Autonomous Wilderness Search and Rescue. IEEE Trans. Cybern. **45**, 1784–1797 (2015). https://doi.org/10.1109/TCYB.2014.2360368
47. Doherty, P.J., Guo, Q., Doke, J., Ferguson, D.: An Analysis of Probability of Area Techniques for Missing Persons in Yosemite National Park. Appl. Geogr. **47**, 99–110 (2014). https://doi.org/10.1016/j.apgeog.2013.11.001
48. Kashino, Z., Kim, J.Y., Nejat, G., Benhabib, B.: Spatiotemporal Adaptive Optimization of a Static-Sensor Network via a Non-Parametric Estimation of Target Location Likelihood. IEEE Sensors J. **17**, 1479–1492 (2017). https://doi.org/10.1109/JSEN.2016.2638623
49. Lin, L., Goodrich, M.A.: A Bayesian Approach to Modeling Lost Person Behaviors Based on Terrain Features in Wilderness Search and Rescue. Comput. Math. Organ. Theory. **16**, 300–323 (2010). https://doi.org/10.1007/s10588-010-9066-2
50. Mohibullah, W., Julier, S.J.: Stigmergic Search for a Lost Target in Wilderness. In: Proc. Sensor Signal Processing Defence. pp. 1–5, London (2011)
51. Sava, E., Twardy, C., Koester, R., Sonwalkar, M.: Evaluating Lost Person Behavior Models. Trans. GIS. **20**, 38–53 (2016). https://doi.org/10.1111/tgis.12143
52. Koester, R.J.: Lost Person Behavior: A Search and Rescue Guide on Where to Look for Land. Air and Water. dbS Productions, Charlottesville (2008)
53. Croft, E.A., Benhabib, B., Fenton, R.G.: Near-time optimal robot motion planning for on-line applications. J. Robot. Syst. **12**, 553–567 (1995). https://doi.org/10.1002/rob.4620120805
54. Macwan, A., Nejat, G., Benhabib, B.: Optimal Deployment of Robotic Teams for Autonomous Wilderness Search and Rescue. In: Proc. IEEE/RSJ Int. Conf. Intell. Robot. Syst. pp. 4544–4549, San Francisco (2011)
55. Tobler, W.: Non-Isotropic Geographic Modeling. Three Present. Geogr. Anal. Model. St. Barbara Natl. Cent. Geogr. Inf. Anal. Univ. Calif. (1993)
56. Bakhtari, A., Naish, M.D., Eskandari, M., Croft, E.A., Benhabib, B.: Active-Vision-Based Multisensor Surveillance – An Implementation. IEEE Trans. Syst. Man Cybern. Part C Appl. Rev. **36**, 668–680 (2006). https://doi.org/10.1109/TSMCC.2005.855525
57. Bakhtari, A., Benhabib, B.: An Active Vision System for Multitarget Surveillance in Dynamic Environments. IEEE Trans. Syst. Man Cybern. Part B Cybern. **37**, 190–198 (2007). https://doi.org/10.1109/TSMCB.2006.883423
58. Shneydor, N.A.: Missile Guidance and Pursuit: Kinematics, Dynamics and Control. Woodhead Publishing (1998)
59. Borg, J.M., Mehrandezh, M., Fenton, R.G., Benhabib, B.: Navigation-Guidance-Based Robotic Interception of Moving Objects in Industrial Settings. J. Intell. Robot. Syst. **33**, 1–23 (2002). https://doi.org/10.1023/A:1014490704273
60. Kunwar, F., Benhabib, B.: Rendezvous-Guidance Trajectory Planning for Robotic Dynamic Obstacle Avoidance and Interception. IEEE Trans. Syst. Man Cybern. Part B Cybern. **36**, 1432–1441 (2006). https://doi.org/10.1109/TSMCB.2006.877792
61. Kunwar, F., Wong, F., Mrad, R.B., Benhabib, B.: Guidance-Based On-Line Robot Motion Planning for the Interception of Mobile Targets in Dynamic Environments. J. Intell. Robot. Syst. **47**, 341–360 (2006). https://doi.org/10.1007/s10846-006-9080-2
62. Hujic, D., Croft, E.A., Zak, G., Fenton, R.G., Mills, J.K., Benhabib, B.: The robotic interception of moving objects in industrial settings: strategy development and experiment. IEEEASME Trans. Mechatron. **3**, 225–239 (1998). https://doi.org/10.1109/3516.712119
63. Rossi, R.J.: Mathematical Statistics: An Introduction to Likelihood Based Inference. Wiley, Hoboken (2018)
64. Julier, S.J., Uhlmann, J.K.: Unscented Filtering and Nonlinear Estimation. Proc. IEEE. **92**, 401–422 (2004). https://doi.org/10.1109/JPROC.2003.823141
65. Search Experiment Example for Aerial Wilderness Search and Rescue with Ground Support, https://www.youtube.com/watch?v=bX0IAm-fRJs

66. Zhao, Q., Zhang, L., Han, Y., Fan, C.: Polishing Path Generation for Physical Uniform Coverage of the Aspheric Surface Based on the Archimedes Spiral in Bonnet Polishing. Proc. Inst. Mech. Eng. Part B J. Eng. Manuf. 0954405419838655 (2019). https://doi.org/10.1177/0954405419838655

Zendai Kashino received the B.A.Sc. degree in engineering physics from the University of British Columbia, Vancouver, BC, Canada, in 2015. He is currently pursuing the Ph.D. degree in mechanical engineering at the University of Toronto under the supervision of Prof. Benhabib and Prof. Nejat, with a focus on autonomous wilderness search and rescue.

Goldie Nejat received the B.A.Sc. and Ph.D. degrees in mechanical engineering from UofT in 2001 and 2005, respectively. She is currently the Canada Research Chair in Robots for Society, and also a Professor and the Director of the Autonomous Systems and Biomechatronics Lab in the Department of Mechanical and Industrial Engineering, UofT. Her research interests include sensing, HRI, semi-autonomous and autonomous control, and intelligence of assistive/service robots for search and rescue, exploration, healthcare, and surveillance applications.

Beno Benhabib received the B.Sc., M.Sc., and Ph.D. degrees all in mechanical engineering in 1980, 1982, and 1985, respectively. He has been a Professor with the Department of Mechanical and Industrial Engineering at the University of Toronto, Toronto, ON, Canada, since 1986. His current research interests include the design and control of intelligent autonomous systems.